

Correlation method for processing speckles of signals from single-fibre multimode interferometers by using charge-coupled devices

Yu.N. Kul'chin, O.B. Vitrik, A.D. Lantsov

Abstract. The correlation method for processing signals from a single-fibre multimode interferometer by using a digital charge-coupled device is studied experimentally and theoretically. Optimal conditions are determined for recording multimode interference patterns with charge-coupled devices. It is found that the nonlinearity of characteristics of such devices affects the results of correlation measurements. The method for eliminating this influence is proposed. The correlation method considered in the paper allows one to measure a linear deformation of the interferometer within 0–80 μm with an accuracy of $\sim \pm 3 \mu\text{m}$ for typical multimode fibres with the core diameter 50 μm .

Keywords: fibre interferometer, correlation method for signal processing, speckle pattern.

One of the most promising schemes of interference fibre transducers (IFTs) for monitoring stressed–strained states of technological objects is the single-fibre multimode interferometer (SFMI) scheme [1], which combines extreme simplicity with high metrological characteristics. A SFMI transducer should extract data on the deformation of a sensitive fibre from a random speckle pattern of multimode interference. This problem was solved in papers [2–4] by using the dependence of the correlation coefficient of speckle fields produced by the SFMI on the phase variations of the modes of a deformed fibre. However, correlation holographic and amplitude transparencies considered in [2–4] require constant rewriting due to the uncontrollable mismatch between a speckle pattern and the reference image recorded in the transparency caused by variations in the temperature of the environment. This prevents the application of these methods in practical measuring systems. It seems that the use of digital electronic devices for recording and processing speckle signals of SFMIs can lead to the solution of this problem upon automation of the reference-image rewriting processes and

increasing the accuracy of correlation calculations. The aim of our paper is to develop and study the method of electronic recording and correlation processing of SFMI signals by using a high-resolution CCD array and PC.

In the method proposed here, the CCD array of a video camera records the reference image of a speckle pattern, which corresponds to the initial state of a fibre in the interferometer. The fibre deformation caused by external perturbations leads to a change in the spatial arrangement of speckles in the pattern recorded with the CCD array. A comparison of speckle signals before and after fibre deformation is performed by the correlation method by using the correlation coefficient, which in the LP mode approximation is described by the expression [2–4]

$$\rho_{12} = \frac{\sin^2(\Delta\Psi_{\max}/2)}{(\Delta\Psi_{\max}/2)^2}, \quad (1)$$

where $\Delta\Psi_{\max}$ is the maximum phase shift between the SFMI modes. It follows from (1) that ρ_{12} depends only on $\Delta\Psi_{\max}$, the value of the correlation coefficient being independent of the initial distribution of speckles in the intermode interference pattern.

The phase shift of the LP_{pq} mode caused by the fibre deformation can be written in the form [1]

$$\Delta\Psi_{pq} = kn_{pq} \frac{dl}{dZ} \Delta Z + kl \frac{dn_{pq}}{dZ} \Delta Z, \quad (2)$$

where $n_{pq} = \beta_{pq}/k$ is the effective refractive index for the LP_{pq} mode; l is the fibre length; β_{pq} is the mode propagation constant; ΔZ is the amplitude of the external deformation action; $k = 2\pi/\lambda$; and λ is the radiation wavelength. We assume here that a deformation change in the effective refractive index for the LP mode can be caused by the axial stretch of the fibre and its small macroscopic bends. The possibility of appearance of microbends and other factors affecting the mode amplitude is not considered. In this case, within the framework of the perturbation theory [5], expression (2) can be rewritten in the form

$$\Delta\Psi_{pq} = kn_{pq} \frac{dl}{dZ} \Delta Z + k\Delta n_{pq} \zeta_{pq} \frac{l}{r_0} \frac{dr_0}{dZ} \Delta Z + kl \frac{d\tilde{n}}{dZ} \Delta Z, \quad (3)$$

where

$$\zeta_{pq} = \frac{2U_{pq}^2}{V^2} \frac{K_p^2(W_i)}{K_{p+1}(W_i)K_{p-1}(W_i)}; \quad U_{pq} = r_0(k^2n_1^2 - \beta_{pq}^2)^{1/2};$$

Yu.N. Kul'chin Presidium of Far East Branch, Russian Academy of Sciences, ul. Svetlanskaya 50, 690014 Vladivostok;
Tel.: +7 (4232) 26 88 90;

O.B. Vitrik, A.D. Lantsov Chair of Physics, Far Eastern State Technical University (V.V. Kuibyshev Far East Polytechnical Institute), Aksakovskii per. 3A, 690010 Vladivostok, Russia;
e-mail: vitrik@mail.primorye.ru, alexeyla@mail.ru

Received 20 October 2005; revision received 12 January 2006
Kvantovaya Elektronika 36 (4) 339–342 (2006)
Translated by M.N. Sapozhnikov

$$W_{pq} = (V^2 - U_{pq}^2)^{1/2}; \quad V = kr_0(n_1^2 - n_2^2)^{1/2};$$

\tilde{n} , n_1 , and n_2 are the refractive indices of the material, fibre core and cladding, respectively; $\Delta n = n_1 - n_2$; r_0 is the fibre core radius; and K_p is the p -order McDonald function. Because the third term in (3) determined by variation in \tilde{n} is the same for all the modes, it has no effect on the maximum phase difference between them. For this reason, temperature variations in the refractive index of the fibre should not affect the results of measuring the correlation coefficient. Taking into account that the fibre elongation leads to a decrease in the fibre core radius, we obtain from (3) and approximate expressions for mode parameters [5] that

$$\Delta\Psi_{\max} = k\Delta n(1 - \mu\tilde{\zeta})\Delta l, \quad (4)$$

where μ is the Poisson coefficient; $\tilde{\zeta} = 2 - \pi/V$; and Δl is the change in the fibre length. By combining expressions (1) and (4), we obtain the expression for the correlation coefficient

$$\rho_{12} = \frac{\sin^2(\pi\Delta l/\Delta l_0)}{(\pi\Delta l/\Delta l_0)^2}, \quad (5)$$

where

$$\Delta l_0 = \frac{\lambda}{\Delta n(1 - \mu\tilde{\zeta})}.$$

Within the framework of our model, the correlation coefficient is determined by a change in the length of the SFMI fibre and is independent of other factors. The dependence $\rho_{12}(\Delta l)$ calculated from (5) for a silica fibre with NA = 0.2, $\Delta n = 0.013$ and the core diameter 50 μm is presented in Fig. 1 [curve (1)].

It follows from these results that there exists such a characteristic increase in the base Δl_0 of a sensitive fibre in the SFMI (equal to 80 μm for the fibre used here) above which a complete decorrelation of the intermode interference signal and reference image is observed. In this case, the

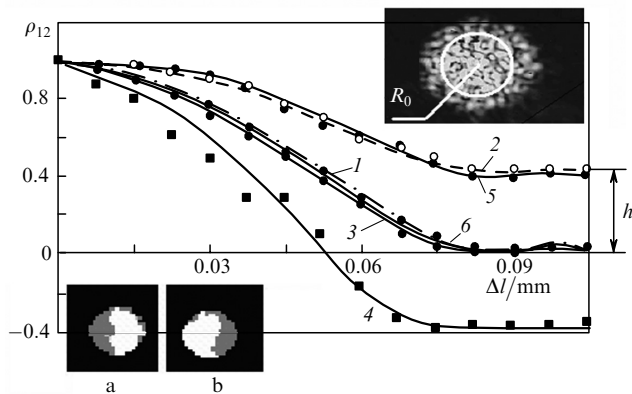


Figure 1. Theoretical (1) and experimental (2–6) dependences of the correlation coefficient ρ_{12} on the fibre elongation Δl for the radius of the picture under study $R = 1.3R_0$ (2), $0.44R_0$ (3) and $0.11R_0$ (4) (R_0 is the radius of the illuminated region within which the CCD array records 80 % of the light power) and for the distribution parameter (see below) $\langle X \rangle / X_{\max} = 0.8$ (5) and 0.15 (6). The upper inset shows the distribution of the intermode interference signal in the detection plane; the lower inset shows the selected initial (a) and final (b) fragments of this signal.

further correlation processing is impossible. If $\Delta l < \Delta l_0$, the correlation coefficient can be high enough for calculating from its measured value a change in the fibre length. When $\rho_{12}(\Delta l) > 0.3$, expression (5) is well approximated by the exponential dependence $\rho_{12} = \exp\{-[\Delta l/(0.42\Delta l_0)]^2\}$. Then, the value of Δl can be calculated from the expression

$$\Delta l = 0.42\Delta l_0(-\ln \rho_{12})^{1/2}, \quad (6)$$

which gives the calculation error no more than 0.1 %.

The obtained results were experimentally verified by using the setup shown in Fig. 2. The deformation of the sensitive fibre in the SFMI was produced by moving mount (6) along the x axis or by moving screw (5) along the y axis. The output optical signal of the SFMI is recorded with the video camera CCD array coupled with a PC.

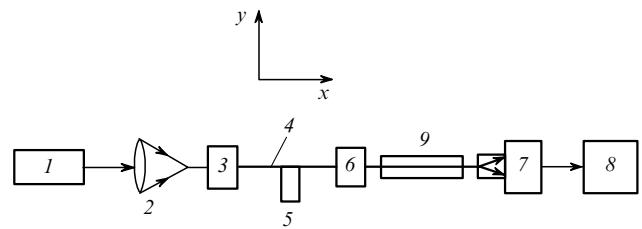


Figure 2. Scheme of the experimental setup: (1) He–Ne laser; (2) microobjective; (3, 6) mounts; (4) SFMI; (5) screw; (6) video camera 320 × 240 pixel CCD array; (8) PC; (9) heated cell with water.

We found during experiments that the conditions of illumination of the CCD array by radiation from the SFMI considerably affect the results of correlation processing. The recorded image, as shown in Fig. 1 (the upper inset) has a circular shape with the indistinct centre and boundary. Because of this, it is necessary to choose artificially the positions of the centre and boundaries during data processing and elucidate the influence of this choice on the measurement results. We found the coordinates of the image centre from the expression similar to the relation for determining the coordinates $x_{\text{cg}}, y_{\text{cg}}$ of the centre of gravity of material bodies, in which the density of a material body at some point is replaced by the intensity I_i :

$$x_{\text{cg}} = \frac{\sum_{i=1}^n x_i I_i(x, y)}{\sum_{i=1}^n I_i(x, y)}, \quad y_{\text{cg}} = \frac{\sum_{i=1}^n y_i I_i(x, y)}{\sum_{i=1}^n I_i(x, y)}.$$

Then, we measured the dependences $\rho_{12}(\Delta l)$ for different radii R of the picture boundary, which are presented in Fig. 1 [curves (2–4)].

It follows from the results obtained that there exists the optimal radius of the picture lying in the range $R_0/3 - R_0$ (where R_0 is the radius of the region where 80 % of the light power is detected with the CCD array). For any value of R lying within the optimal range, the dependence $\rho_{12}(\Delta l)$ [curve (3) in Fig. 1] is close to the calculated one. For the case $R < R_0/3$, the correlation coefficient takes negative values [curve (4)]. This can be explained by the correlated rearrangement of individual speckles at a small size of the region of the interference pattern selected for processing [6]. Indeed, if a single light spot is recorded within such a region,

which gradually moves from the right part of the region to the left one due to correlated rearrangement, the final image of the region will be anti-correlated with the initial one (Fig. 1, photographs a and b, respectively, in the lower inset). When $R_0/3 \leq R \leq R_0$, many speckles are recorded, whose mutual movement is not correlated. In this case, the correlation coefficient decreases to zero during fibre stretching. If $R \geq R_0$, the CCD array records regions outside the speckle pattern, whose brightness is independent of the SFMI length. As a result, the correlation coefficient decreases down to some positive value h , as illustrated by curve (2) in Fig. 1. Figure 3 shows the measured dependence of the parameter h on R .

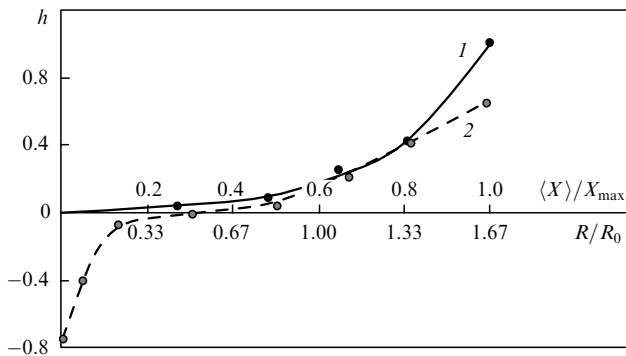


Figure 3. Dependences of the mismatch parameter h for the experimental and calculated curves on the distribution parameter $\langle X \rangle / X_{\max}$ (1) and the chosen radius R/R_0 (2) of the picture boundary.

The light intensity at different points of the intermode interference pattern is a random quantity and can considerably exceed the average level at some points. As a result, some of the pixels of the CCD array can be in a nonlinear detection regime, which in turn affects the results of correlation calculations. To elucidate the contribution of such pixels, we measured the statistical characteristics of the light intensity distribution in the image recorded with the CCD array. We found that, as the radiation power incident on the SFMI was increased, the distribution parameter $\langle X \rangle / X_{\max}$ increased monotonically from 0 to 1 (where X is the detected radiation intensity, which can be not directly proportional to the incident light intensity because of the CCD array nonlinearity, X_{\max} is the maximum value of the detected intensity, and the angle brackets denote the average value of the random quantity). Upon recording weak light fluxes from the SFMI, when $\langle X \rangle / X_{\max} \leq 0.15$, the measured radiation intensity density $dP(X)/dX$ in the speckle pattern obeys the exponential law [Fig. 4, curve (1)]. Because the probability density for the light intensity distribution in a random coherent field should have namely this type [7], this demonstrates a linear detection regime. In the given case, the correlation coefficient behaves according to (5), which is illustrated by curve (6) in Fig. 1.

For $\langle X \rangle / X_{\max} > 0.15$, the maximum of the intensity distribution density in Fig. 4 [curves (2–5)] shifts to the right towards $X = X_{\max}$. This occurs because at high illumination intensities the probability of finding a pixel of the CCD array in the nearly saturated state increases and indicates that the recording regime is nonlinear. In this case, the type of the dependence $\rho_{12}(\Delta l)$ also changes, which is

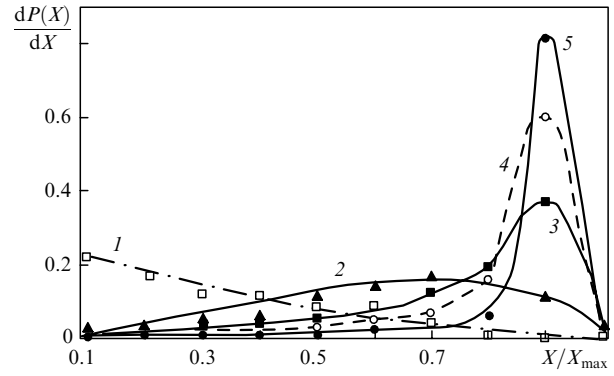


Figure 4. Light intensity distribution densities $dP(X)/dX$ for $\langle X \rangle / X_{\max} = 0.15$ (1), 0.18 (2), 0.4 (3), 0.48 (4) and 0.84 (5).

illustrated by curve (5) in Fig. 1. One can see that ρ_{12} decreases down to a constant value $h > 0$, which can distort the results of measuring the fibre elongation. In this case, it is necessary to use optical filters to attenuate the light flux coupled to the SFMI until the acceptable ratio $\langle X \rangle / X_{\max}$ is obtained. Therefore, the statistical approach allows one to obtain the linear operation regime of the CCD array without direct measurements of the nonlinearity parameters of its pixels and the incident light intensity. Curve (1) in Fig. 3 shows the measured dependence of h on the ratio $\langle X \rangle / X_{\max}$.

To verify the above conclusion on the independence of the measured value of the correlation coefficient on the initial light intensity distribution in the pattern produced by the SFMI, we measured the dependence $\rho_{12}(\Delta l)$ by using different reference images. The results are presented in Fig. 5 [curves (1–4)]. One can see that these dependences are coincident as a whole. The observed scatter is explained by the statistical character of the measured parameter and is the source of the measurement error of Δl . This error can achieve $\pm 3 \mu\text{m}$ for fibres of the type under study. By averaging the data on the fibre elongation obtained by using simultaneously several reference images, the measurement error can be considerably reduced. For this purpose, we compared the current state of the speckle pattern with a set of reference images recorded for three fixed positions of mount (6) measures with a high accuracy (Fig. 2). Our experiments showed that the root-mean-square deviation of the measurement result did not exceed $0.35 \mu\text{m}$. However, the corresponding calculations required a longer computer time (up to 380 ms per frame processing as compared to 95 ms when a single reference image was used).

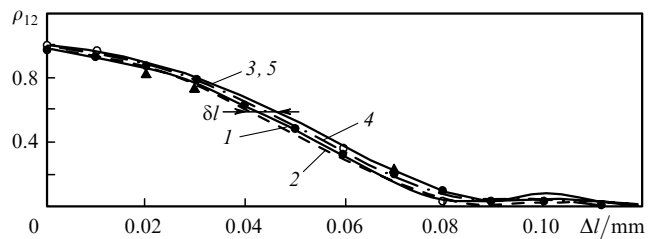


Figure 5. Dependences $\rho_{12}(\Delta l)$ obtained by using different reference images directly upon the axial stretch of the fibre (1–4) and upon the fibre stretch caused by sagging of the stretched fibre.

To elucidate the influence of temperature on the measurements of the SFMI elongation, the SFMI fibre of length 0.1 m was placed into a cell with water (as shown in Fig. 2) heated from 15 to 60 °C. As a result, we found experimentally that the temperature measurement error of the relative elongation of the SFMI in the above temperature range was $7.3 \times 10^{-7} \text{ }^\circ\text{C}^{-1}$. This value almost coincide with the temperature expansion coefficient for pure silica equal to $5.5 \times 10^{-7} \text{ }^\circ\text{C}^{-1}$ (the difference is probably explained by the influence of a polymer cladding of the fibre). This confirms the conclusion that the result of correlation processing depends only on the temperature change in the fibre length rather than on the temperature dependence of the refractive index of the fibre material.

To study the effect of the fibre bends on the measured value of the correlation coefficient, we subjected SFMI fibre (4) (Fig. 2) simultaneously to bending and tensile strains by moving screw (5) transversely. The dependence $\rho_{12}(\Delta l)$ obtained in this way is shown in Fig. 5 [curve (5)]. One can see that this curve coincides within the measurement error with the dependence measured directly during the axial stretch of the fibre [Fig. 5, curve (1)]. This means that the fibre bend does not affect the results of measuring the correlation coefficient.

As mentioned above, the quantitative measurements of the SFMI elongation can be performed if the correlation coefficient is sufficiently high. This condition can be provided in measurements of large fibre stretches by rewriting the reference signal in the computer memory each time when the correlation coefficient decreases down to a certain threshold value (for example, down to $\rho_{12} = 0.6$ in our case). The quadratic character of the dependence $\rho_{12}(\Delta l)$ leaves the uncertainty in the sign of the measured fibre elongation.

We determined the sign of Δl by using the 'double count' algorithm, when the current intensity distribution $I_2(x, y)$ in the speckle pattern is compared with no less than two reference images, of which the second one remains in the computer memory after the last rewriting cycle. Let us assume that $I_1(x, y)$ is the current reference distribution replacing the previous distribution $I_0(x, y)$ at the instant when the correlation coefficient achieved the threshold value 0.6, ρ_{12} is the correlation coefficient of the distributions $I_2(x, y)$ and $I_1(x, y)$ and ρ_{20} is the correlation coefficient of the distributions $I_2(x, y)$ and $I_0(x, y)$. We will use the correlation coefficient ρ_{21} to calculate Δl from (6) and ρ_{20} to determine the elongation sign. If $\rho_{20} < 0.6$, the deviation of the distribution $I_2(x, y)$ from $I_0(x, y)$ continues to increase and $\Delta l > 0$, whereas if $\rho_{20} > 0.6$, we have $\Delta l < 0$.

By using this approach, we can measure the SFMI elongations as large as is wished (up to the fibre rupture) and determine the elongation sign (stretch or compression). The results of these measurements are presented in Fig. 6, where curve (1) corresponds to variations in the fibre length caused by the back-and-forth micrometer-controlled motion of movable mount (6) (Fig. 2) and curve (2) corresponds to measurements of the fibre elongation obtained after correlation processing. One can see that these curves coincide within the measurement error.

Thus, the method proposed in the paper provides the high-accuracy monitoring of absolute variations in the fibre length in the range restricted by the mechanical strength of the fibre. The method ensured the high temperature stability and can be used for the development of highly efficient

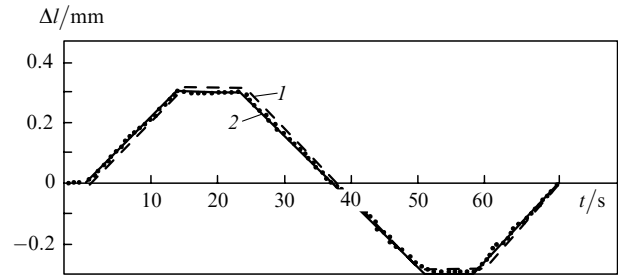


Figure 6. Dependences of variations in the fibre length measured with a micrometer (1) and by the correlation method (2).

systems for monitoring linear deformation of technogenous objects.

References

1. Busurin B.I., Nosov Yu.R. *Volokonno-opticheskie datchiki* (Fibre Sensors) (Moscow: Energoatomizdat, 1990).
2. Kul'chin Yu.N., Bykovskii Yu.A., Vitrik O.B., Larkin A.I. *Kvantovaya Elektron.*, **17**, 95 (1990) [*Sov. J. Quantum Electron.*, **20**, 83 (1990)].
3. Kul'chin Yu.N., Vitrik O.B., Maksaev O.G., Kirichenko O.V., Kamenev O.T. *Zh. Tekh. Fiz.*, **66**, 137 (1996).
4. Kul'chin Yu.N., Vitrik O.B., Kirichenko O.V., Kamenev O.T., Petrov Yu.S., Maksaev O.V. *Opt. Eng.*, **36**, 1494 (1997).
5. Snyder A., Love J. *Optical Waveguide Theory* (London: Chapman & Hall, 1983; Moscow: Radio i Svyaz', 1980).
6. Kul'chin Yu.N., Bykovskii Yu.A., Obukh V.F., Smirnov V.L. *Kvantovaya Elektron.*, **17**, 1080 (1990) [*Sov. J. Quantum Electron.*, **20**, 996 (1990)].
7. Goodman J. *Statistical Optics* (New York: Wiley & Sons, 1985; Moscow: Mir, 1988).